

# The Chemistry of an $N^5$ -Methyl-1,5-dihydroflavin and Its Aminium Cation Radical

Cemal Kemal<sup>1</sup> and Thomas C. Bruice\*

Contribution from the Department of Chemistry, University of California, Santa Barbara, California 93106. Received November 3, 1975

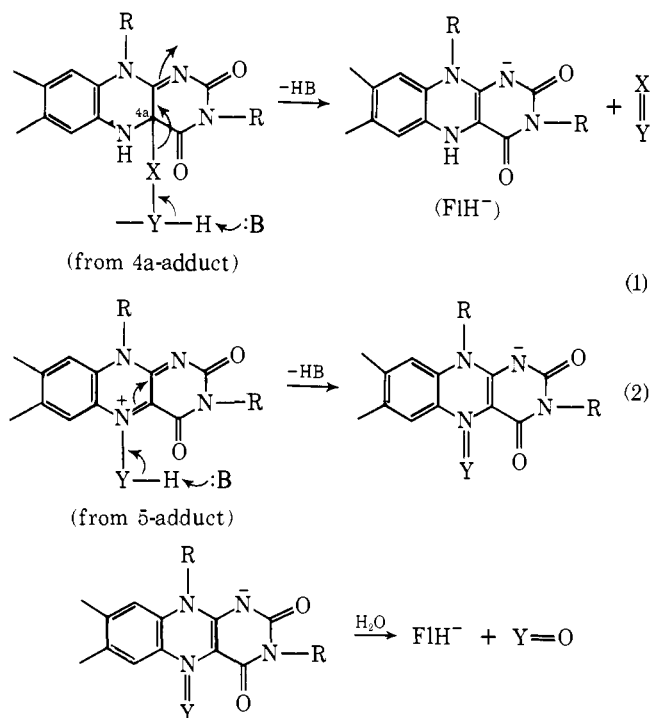
**Abstract:** 3,5-Dimethylflumiflavin ( $\text{Fl}_{\text{ox}}^+\text{CH}_3$ ) undergoes general-base-catalyzed ( $\beta = 0.6$ )  $N^5$ -methyl proton loss at pH values below 8. At more basic pH values,  $\text{HO}^-$ -mediated hydrolysis of the isoalloxazine ring structure of the pseudo base ( $\text{FlOHCH}_3$ ) occurs. The  $\text{pK}_a$  associated with pseudo-base formation has been determined to be 4.15 by employing the hydrolytically more stable deuterio analogue ( $\text{Fl}_{\text{ox}}^+\text{CD}_3$ ). The following observations pertain to the general-base-catalyzed reaction (below pH 8). No exchange of -D for -H at the  $N^5$ - $\text{CH}_3$  group can be detected when solvolysis is carried out in  $\text{D}_2\text{O}$ . The kinetic deuterium isotope effect (i.e.,  $\text{Fl}_{\text{ox}}^+\text{CH}_3/\text{Fl}_{\text{ox}}^+\text{CD}_3$ ) is 10.5 and 14.0 when the general bases are  $\text{H}_2\text{O}$  and  $\text{CH}_3\text{CO}_2^-$ , respectively. A kinetic solvent deuterium isotope effect ( $k_{\text{Fl}_{\text{ox}}^+\text{CH}_3, \text{H}_2\text{O}}/k_{\text{Fl}_{\text{ox}}^+\text{CH}_3, \text{D}_2\text{O}}$ ) of 2.0 is obtained when  $\text{H}_2\text{O}$  and  $\text{D}_2\text{O}$  serve as general base. The rate constant for  $\text{HO}^-$ -mediated proton abstraction from  $\text{Fl}_{\text{ox}}^+\text{CH}_3$  is comparable to that when ethyl nitroacetate or acetylacetone serve as substrates and exceeds that for  $\text{C}(8\alpha)\text{-H}$  proton abstraction from FMN by  $10^3$  to  $10^4$ . The overall mechanism of Scheme III is proposed to account for these observations as well as the rather unique kinetics and the products obtained. In Scheme III, the rate-determining general base proton abstraction from  $\text{Fl}_{\text{ox}}^+\text{CH}_3$  yields the formaldehyde imine of dihydroflavin (IM), which yields the carbinolamine ( $\text{FlH-CH}_2\text{OH}$ ), which in turn dissociates to dihydroflavin ( $\text{FlH}_2$ ) and  $\text{CH}_2\text{O}$ . Both  $\text{FlH-CH}_2\text{OH}$  and  $\text{FlH}_2$  undergo one-electron ( $1e^-$ ) transfers to  $\text{Fl}_{\text{ox}}^+\text{CH}_3$  to yield the radical products ( $\text{FlCH}_3\cdot + \text{FlCH}_2\text{OH}\cdot$ ) and ( $\text{FlCH}_3\cdot + \text{FlH}\cdot$ ), respectively. The radical species  $\text{FlCH}_2\text{OH}\cdot$  undergoes, in turn, both a second  $1e^-$  transfer to  $\text{Fl}_{\text{ox}}^+\text{CH}_3$  and loss of  $\text{CH}_2\text{O}$  to yield  $\text{FlH}\cdot$ , which then transfers  $1e^-$  to  $\text{Fl}_{\text{ox}}^+\text{CH}_3$ . The final products of the reaction are  $(\text{H}_2\text{CO}):(\text{FlCH}_3):\text{Fl}_{\text{ox}} = 1:2:1$ . In agreement with the proposed rapid  $1e^-$  transfer reactions are the observations, in separate experiments, of very rapid reactions between both  $\text{FlH-CH}_2\text{OH}$  and  $\text{FlH}_2$  with  $\text{Fl}_{\text{ox}}^+\text{CH}_3$  to yield  $\text{Fl}_{\text{ox}}$  and  $\text{FlCH}_3\cdot$ . The rate laws derived from Scheme III require the experimentally determined rate constant to be three times that for the H abstraction from the  $\text{CH}_3$  moiety of  $\text{Fl}_{\text{ox}}^+\text{CH}_3$  and further predicts that the rapid recycling of intermediate  $\text{FlCH}_3\cdot$  to  $\text{Fl}_{\text{ox}}^+\text{CH}_3$  should result in a decrease of the overall rate by three times. In the presence of benzoquinone as a  $1e^-$  acceptor the determined rate constant is found to be one-third that obtained in its absence. The solvolysis of  $\text{FlCH}_3\cdot$  is found to be second order in this species, suggesting the intermediacy of the complex  $(\text{FlCH}_3\cdot)_2$ . However, the ensuing reaction is no ordinary radical disproportionation. The kinetic deuterium isotope effect of  $(k_{\text{FlCH}_3\cdot}/k_{\text{FlCD}_3\cdot}) = 13$  at pH 5.0. Though this very large isotope effect dictates that C-H bond breaking is occurring in the critical transition state (as in the case of  $\text{Fl}_{\text{ox}}^+\text{CH}_3$  solvolysis) the rate of  $\text{FlCH}_3\cdot$  disappearance is not influenced by either pH (2.0 to 8.0); the isoalloxazine nucleus of  $\text{FlCH}_3\cdot$  is disrupted by  $\text{HO}^-$ -mediated hydrolysis above pH 8) or the concentration of buffer bases (unlike proton abstraction from  $\text{Fl}_{\text{ox}}^+\text{CH}_3$ ). The deuterium solvent kinetic isotope effect for disappearance of  $\text{FlCH}_3\cdot$  was found to be smaller (i.e., 1.3) than that determined for  $\text{Fl}_{\text{ox}}^+\text{CH}_3$ . There is proposed a  $1e^- + \text{H}^+$  or  $\text{H}\cdot$  intracomplex transfer from the methyl moiety of one  $\text{FlCH}_3\cdot$  species to the other within the initially formed dimeric complex  $(\text{FlCH}_3\cdot)_2$  to yield  $\text{FlH}_2 + \text{FlHCH}_3 + \text{CH}_2\text{O}$  (Scheme IV). In rapid following reactions,  $\text{FlH}_2$  reacts with  $\text{FlCH}_3\cdot$  to yield  $\text{FlH}\cdot + \text{FlHCH}_3$  and the reaction is terminated by  $1e^-$  transfer from  $\text{FlH}\cdot$  to  $\text{FlCH}_3\cdot$  to yield  $\text{Fl}_{\text{ox}} + \text{FlHCH}_3$ . In separate experiments, the reaction of  $\text{FlH}_2$  ( $2.06 \times 10^{-5}$  M) with  $\text{FlCD}_3\cdot$  ( $6.14 \times 10^{-5}$  M) to yield  $\text{Fl}_{\text{ox}} + 2\text{FlHCD}_3$  occurred during the time of manual mixing. Interestingly,  $\text{Fl}_{\text{ox}}$  and  $\text{FlHCH}_3$  either do not react or do so at a very slow rate.

## Introduction

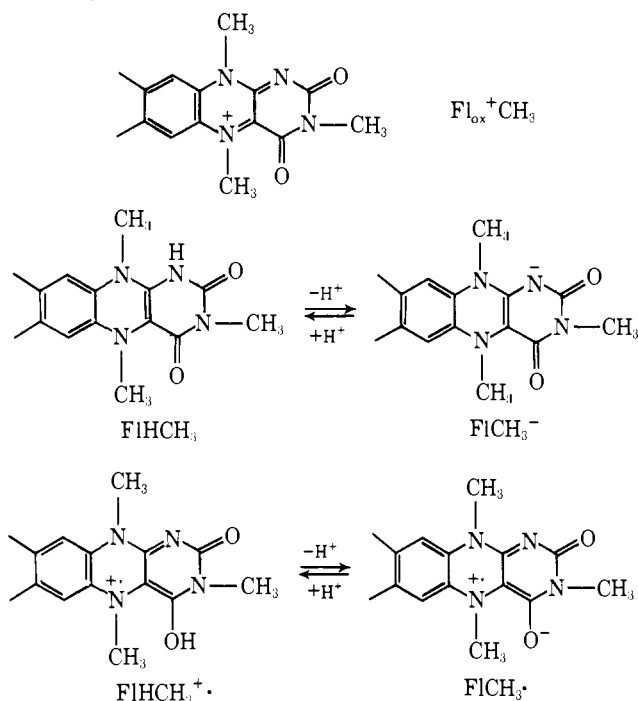
The two-electron ( $2e^-$ ) oxidation or reduction of one substrate by another may occur via consecutive one-electron ( $1e^-$ ) transfer reactions or through a  $2e^-$  addition-elimination reaction.<sup>2</sup> The general mechanism for flavine-mediated oxidation-reduction reactions have been suggested by Hemmerich<sup>3</sup> and Hamilton<sup>4</sup> to involve  $2e^-$  transfer through formation of 5- and 4a-adducts. According to these authors, stepwise  $1e^-$  processes (radical reactions) are to be discounted. Regardless of the validity of the latter suggestion,<sup>5</sup> it is of considerable value to obtain a sound understanding of the chemistry of alkyl 4a- and 5-adducts. Base-catalyzed E2 and E1cB eliminations of alkyl substituents from the 5 and 4a positions may be formulated (eq 1 and 2). A preliminary account of studies of a model system for the process of eq 1 has appeared.<sup>6</sup> The present study deals with the solution chemistry of 3,5-dimethylflumiflavin ( $\text{Fl}_{\text{ox}}^+\text{CH}_3$ ) and its  $1e^-$  ( $\text{FlHCH}_3^+ + \text{FlCH}_3\cdot$ ) and  $2e^-$  ( $\text{FlHCH}_3 + \text{FlCH}_3^-$ ) reduction products (Scheme I).

## Experimental Section

**Materials.** 3,5-Dimethyl-1,5-dihydroflumiflavin ( $\text{FlHCH}_3$ ) and 3,5-dimethylflumiflavin perchlorate ( $\text{Fl}_{\text{ox}}^+\text{CH}_3$ ) were prepared as described by Ghisla et al.<sup>7</sup> 5-Trideuteriomethyl analogues of the above flavins were made by the same procedure utilizing dimethyl- $d_6$  sulfate (99% Aldrich).  $N^5$ -Methylmonohydroflumiflavin ( $\text{FlCH}_3\cdot$ ) was prepared in situ by one of the three following methods: (1) from  $\text{Fl}_{\text{ox}}^+\text{CH}_3$



Scheme 1



solvolysis under anaerobic conditions [ $FlCH_3^-$  produced in this manner is in the presence of  $Fl_{ox}$  ( $FlCH_3^-/Fl_{ox} = 2.0$ ; see Results)]; (2) by comproportionation [solutions containing equimolar amounts of  $Fl_{ox}^+CH_3$  and  $FlHCH_3$  were mixed;  $FlCH_3^-$  forms quantitatively during mixing time (at neutral pH's or below)]; (3) by bubbling  $O_2$  through an  $FlHCH_3$  solution for a few seconds and then deaerating the solution. Since some  $Fl_{ox}^+CH_3$  is also produced and is converted to a mixture of  $Fl_{ox}$  and  $FlCH_3^-$  (during deoxygenation time >30 min), the radical produced by this method is also contaminated with  $Fl_{ox}$ , though the amount of  $Fl_{ox}$  is not as great as obtained with method 1.  $FlCD_3^-$  was made analogously using  $Fl_{ox}^+CD_3$  and/or  $FlHCD_3$ . Ninhydrin and benzoquinone were of analytical grade (Calbiochem).

**Kinetic Measurements.** All kinetic experiments reported in this paper were carried out at  $30 \pm 0.2^\circ$  in doubly glass distilled water through which argon (scrubbed of traces of  $O_2$  by passing through a vanadous trap<sup>8</sup>) was bubbled for 45 min. Except where noted, the ionic strength was maintained at 1.0 with KCl. Kinetic studies in the absence of buffers were done using a radiometer pH-stat assembly specifically designed<sup>9</sup> for a Cary 15 spectrophotometer. The cell compartment portion of the Cary 15 was contained in a large glove box under a nitrogen atmosphere. In this manner the mixing of solutions as well as the kinetic measurements could be carried out in the pH-stat cell or stoppered cuvettes under a nitrogen atmosphere. Solvolysis of  $Fl_{ox}^+CH_3$  was initiated by dissolving a weighed amount of  $[Fl_{ox}^+CH_3]ClO_4^-$  in a small amount of water (usually ca. 0.2 ml) and immediately adding a portion (0.1 ml) to 25 ml of 1 M KCl solution which had been thermostated at  $30^\circ$  for 30 min in the pH-stat cell compartment. The pH of the solution was rapidly adjusted to the desired value and the progress of the reaction monitored at an appropriate wavelength (550, 430, and 357 nm below pH 4.5; 585 and 447 nm above). When buffers were used, a similar procedure (in the glove box) was followed with fast reactions ( $t_{1/2} < 30$  min): 2 ml of buffer solution contained in a 1-cm path length cuvette was thermostated at  $30^\circ$  in the cell compartment (ca. 15 min), and then 0.1 ml of water solution of  $Fl_{ox}^+CH_3$ , prepared immediately before initiation of reaction, was added. Oxygen free argon<sup>8</sup> was bubbled through the solution for a few seconds to achieve rapid mixing. Final concentrations of  $Fl_{ox}^+CH_3$  were ca.  $10^{-4}$  M when buffers were present and as low as  $10^{-5}$  M without buffers (pH-stat cell path length  $\approx 3.3$  cm). Thunberg cuvettes were used for slow reactions. Typically, a weighed amount of  $[Fl_{ox}^+CH_3]ClO_4^-$  was placed in the upper bulb and 3–5 ml of buffer was placed in the bottom cuvette. The buffer solution was deaerated with argon for at least 1 h and the reaction was initiated by dissolving the crystals by shaking. For these runs a Cary Model 118C spectrophotometer was used. The solvolysis of the radical,  $FlCH_3^-$ , was also studied using Thunberg cuvettes. Comproportionation re-

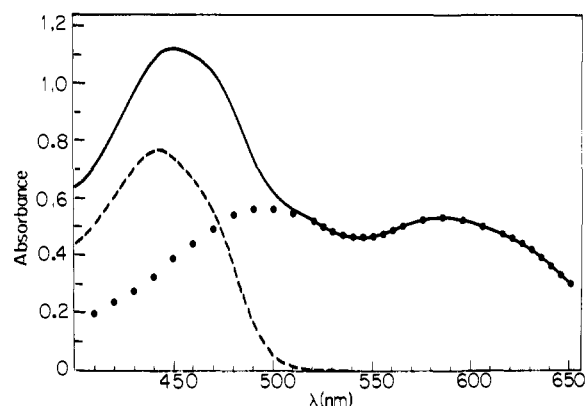


**Figure 1.** (—) Spectrum obtained at the end of the solvolysis of  $1.98 \times 10^{-4}$  M  $Fl_{ox}^+CH_3$  (pH 5.0, 0.25 M acetate). The solid line can be resolved into two components:  $6.35 \times 10^{-5}$  M  $Fl_{ox}$  (---) and  $1.27 \times 10^{-4}$  M  $FlCH_3^-$  (· · ·).

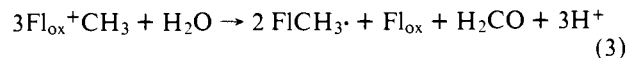
actions, etc., were followed in much the same manner as the solvolysis reactions.

**pK<sub>a</sub> determinations** of  $FlCH_3^-$ ,  $FlCD_3^-$ , and  $Fl_{ox}^+CD_3$  (for pseudo-base formation) were carried out by spectrophotometric titration under the kinetic conditions previously described at 585, 585, and 550 nm, respectively. The experimental absorbance vs. pH plots were fitted to a theoretical sigmoid curve and pK<sub>a</sub>'s of 4.15 ( $Fl_{ox}^+CD_3$ ) and 2.65 ( $FlCH_3^-$  and  $FlCD_3^-$ ) were obtained. The pK<sub>a</sub> of  $Fl_{ox}^+CH_3$  could not be determined due to competing solvolysis. (It was assumed to be 4.15.) pH readings were made with a Radiometer pH meter.

**Formaldehyde Analysis.** Five standard solutions of formaldehyde  $6.8 \times 10^{-5}$ – $3.4 \times 10^{-4}$  M,  $\mu = 1$  KCl, pH 12.5) were prepared and the peak height at  $-1.67$  V was measured on pulsed polarography mode at  $25^\circ C$  ( $\epsilon_{1/2}$  of  $H_2CO = -1.67$  V) using a Princeton Applied Research Model 174 polarograph.  $Fl_{ox}^+CH_3$  (ca.  $3 \times 10^{-4}$  M) solvolysis was allowed to go to completion at pH 2.04 (HCl,  $\mu = 1$  KCl), and then the pH of the solution was changed to 12.5 by addition of a few drops of 10 M KOH and the polarograph recorded. The peak height at  $-1.67$  V was corrected for flavin background and the concentration of formaldehyde was determined by comparison to the standards. The concentration of the formaldehyde solution used to make the standards was determined by the sodium sulfite titration method.<sup>10</sup>

## Results

**Solvolysis of  $Fl_{ox}^+CH_3$  under anaerobic conditions (pH 1–8)** exhibited excellent pseudo-first-order kinetics, yielding a 2:1 mixture of the two flavin species,  $FlCH_3^-$  and  $Fl_{ox}$ , as well as formaldehyde. The stoichiometry of the reaction is given by



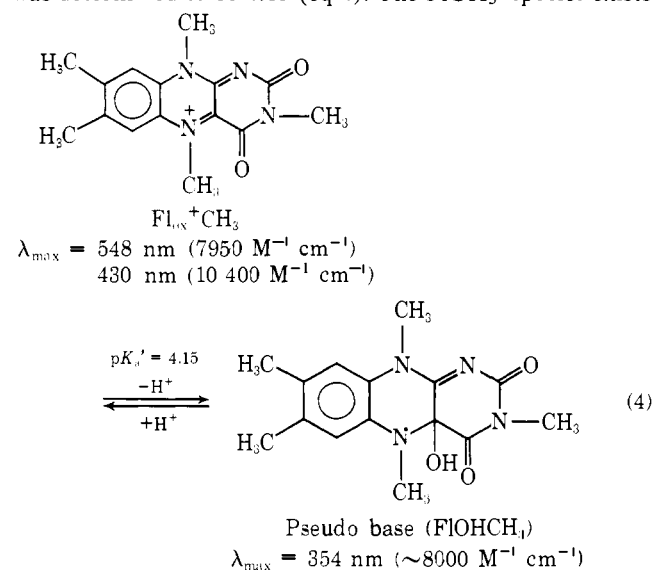
The concentration of flavin products as well as their ratio was determined spectrally (Figure 1). Formaldehyde was quantitated by pulsed polarography. For the latter purpose, the reaction mixture was oxygenated after completion to recycle  $FlCH_3^-$  back to  $Fl_{ox}^+CH_3$ . In this manner all  $FlCH_3^-$  could be converted to  $Fl_{ox}$  and  $H_2CO$ . The yield of  $H_2CO$  was identical when determined in this manner or by carrying out the reaction aerobically and was found to be 100% of  $Fl_{ox}^+CH_3$  consumed (Table I). From a knowledge of the yield of  $FlCH_3^-$ , it can be inferred that the yield of  $H_2CO$ , under anaerobic conditions, is 33.3% of  $Fl_{ox}^+CH_3$  consumed as depicted in eq 3. Keeping reaction solutions anaerobic throughout, it was found that the main product of  $Fl_{ox}^+CH_3$  solvolysis,  $FlCH_3^-$ , was consumed (Figure 2) in a following slower reaction. This second reaction was studied separately and will be taken up later. Spectral changes observed during the solvolysis of  $Fl_{ox}^+CH_3$  (pH 3.05 with HCl) are shown in Figure 3. Tight isobestics are held at 621, 495, 455, 381, and 302 nm, indicating that no intermediates are built up (the same considerations apply to

**Table I.** Results for Formaldehyde Determination by Pulsed Polarography<sup>a</sup>

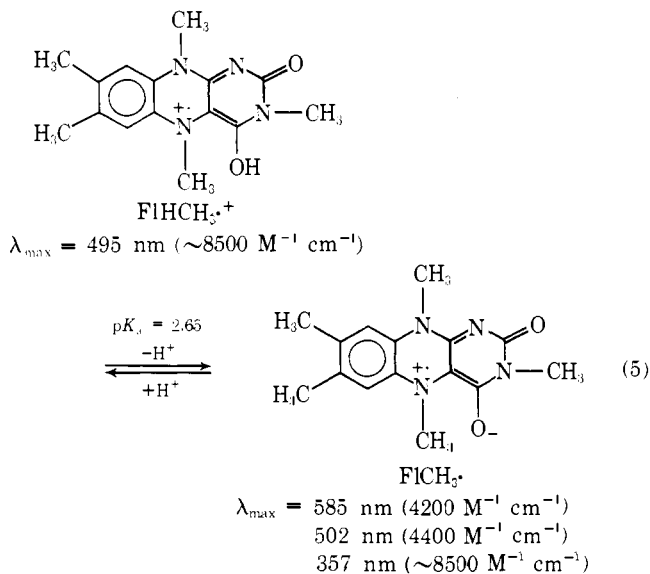
Reaction no.	[Fl <sub>ox</sub> <sup>+</sup> CH <sub>3</sub> ] at start	[Fl <sub>ox</sub> ] <sup>b</sup> found	[H <sub>2</sub> CO] <sup>a</sup> found
1 <sup>c</sup>	3.23 × 10 <sup>-4</sup>	3.19 × 10 <sup>-4</sup>	3.34 × 10 <sup>-4</sup>
2 <sup>d</sup>	3.15 × 10 <sup>-4</sup>	3.08 × 10 <sup>-4</sup>	3.25 × 10 <sup>-4</sup>
3 <sup>e</sup>		1.53 × 10 <sup>-4</sup>	1.36 × 10 <sup>-4</sup>

<sup>a</sup> Fl<sub>ox</sub><sup>+</sup>CH<sub>3</sub> solvolysis was allowed to go to completion at pH 2.0. At the end of the reaction, the pH was adjusted to 12.5, N<sub>2</sub> bubbled through for ca. 15 min, and the polarogram recorded.  $\mu = 1$  with KCl, 25 °C. <sup>b</sup> Determined from its spectrum using  $\epsilon_{443} = 12\,000\text{ M}^{-1}\text{ cm}^{-1}$ . <sup>c</sup> Fl<sub>ox</sub><sup>+</sup>CH<sub>3</sub> solvolysis was allowed to go to completion in O<sub>2</sub> saturated solution. <sup>d</sup> First phase of Fl<sub>ox</sub><sup>+</sup>CH<sub>3</sub> solvolysis was done under anaerobic conditions, then O<sub>2</sub> was bubbled through the solution for 30 min. <sup>e</sup> Same procedure as in <sup>d</sup> was followed. The pulsed polarographic determination of CH<sub>2</sub>O was carried out at pH 12.3.

Fl<sub>ox</sub><sup>+</sup>CD<sub>3</sub>). In aqueous solution, Fl<sub>ox</sub><sup>+</sup>CH<sub>3</sub> is in equilibrium with its pseudobase.<sup>7</sup> The pK<sub>a</sub>' associated with this equilibrium was determined to be 4.15 (eq 4). The FICH<sub>3</sub>· species exists



as a cationic or neutral zwitterionic radical whose pK<sub>a</sub> was determined to be 2.65 (eq 5). Since each acid-base species of



Fl<sub>ox</sub><sup>+</sup>CH<sub>3</sub> and FICH<sub>3</sub>· possesses individual spectral characteristics, the reaction was monitored at a number of wave-

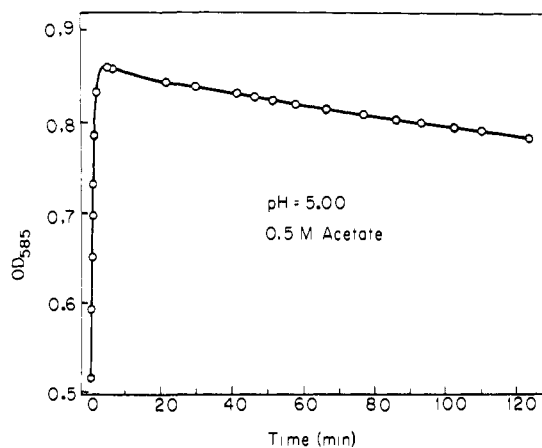


**Figure 2.** Absorbance (585 nm) vs. time plot for Fl<sub>ox</sub><sup>+</sup>CH<sub>3</sub> (1st phase) and FICH<sub>3</sub>· (2nd phase) solvolysis (pH 5.0, 0.5 M acetate, [Fl<sub>ox</sub><sup>+</sup>CH<sub>3</sub>] = 3.1 × 10<sup>-4</sup> M). The radical which is produced from Fl<sub>ox</sub><sup>+</sup>CH<sub>3</sub> by a first-order process disappears in a slower reaction which obeys second-order kinetics (in FICH<sub>3</sub>·).

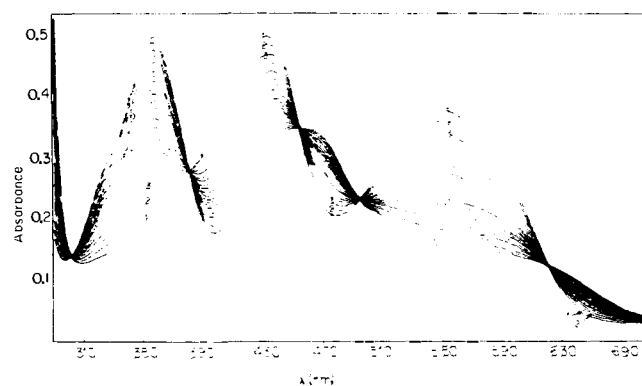


**Figure 3.** Repetitive scan of the solvolysis of Fl<sub>ox</sub><sup>+</sup>CH<sub>3</sub> (5 × 10<sup>-5</sup> M) at pH 3.05 (HCl). Time intervals between successive scans are not equal (scan 1 through 15 every 15 min, 15–18 every 10 min, 18–20 every 20 min, scan 21, 30 min after scan 20).

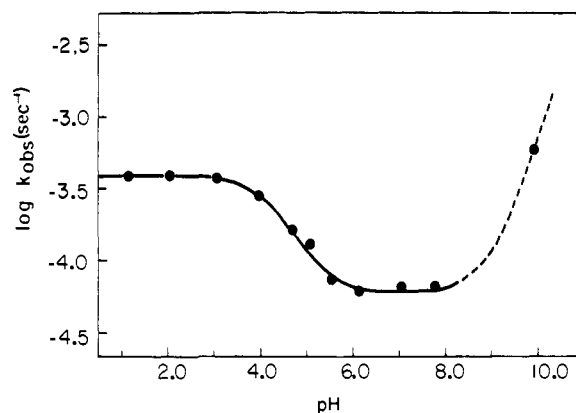


**Figure 4.** Log  $k_{\text{obsd}}$  vs. pH plot for the reaction of (Fl<sub>ox</sub><sup>+</sup>CH<sub>3</sub> ⇌ FIOHCH<sub>3</sub>) with lyate species: (—) solvolysis, (---) hydrolysis.

lengths (550, 430, and 357 nm below pH 4.5; 585, 447 nm above). As the isobestics of Figure 3 suggest, the same pseudo-first-order rate constant is obtained whatever wavelength is monitored at any given pH and buffer concentration.

The pH-log  $k_{\text{obsd}}$  profile for the reaction of Fl<sub>ox</sub><sup>+</sup>CH<sub>3</sub> with lyate species is provided in Figure 4. The data points (with the exception of one point at pH 9.93, which will be discussed later) were obtained spectrally with pH maintained by use of a pH

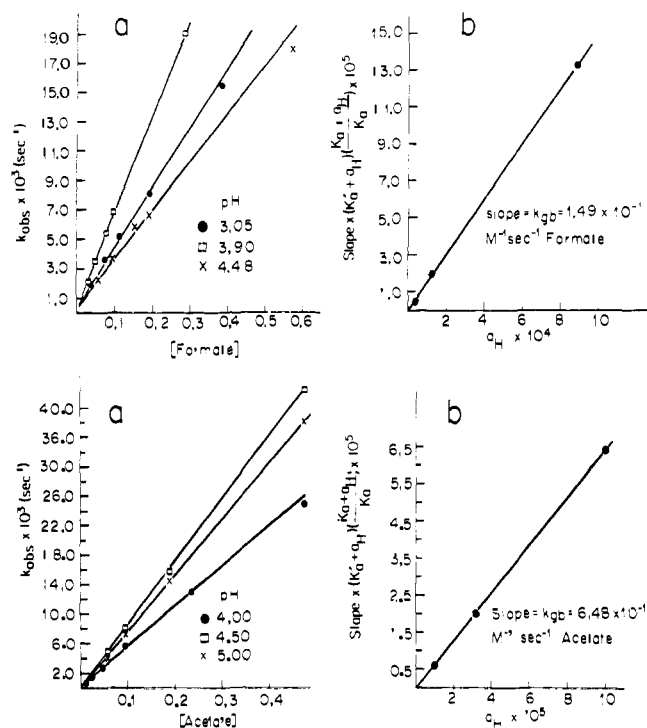


Figure 5. (a) Observed first-order rate constants for the solvolysis of  $\text{Fl}_{\text{ox}}^+\text{CH}_3$  as a function of buffer concentration and pH. (b) Secondary plots for obtaining second-order general base rate constants (see text).

stat and in the absence of buffer. The theoretical solid line of Figure 4 was generated by use of the equation

$$k_{\text{obsd}} = \left( k_0 + k_{\text{HO}} \frac{K_{\text{w}}}{a_{\text{H}}} \right) \frac{a_{\text{H}}}{K_{\text{a}}' + a_{\text{H}}} \quad (6)$$

where  $a_{\text{H}}$  is the hydrogen ion activity determined at the glass electrode,  $k_0 = 3.55 \times 10^{-4} \text{ s}^{-1}$ ,  $k_{\text{HO}} = 2 \times 10^5 \text{ M}^{-1} \text{ s}^{-1}$ ,  $K_{\text{w}} = 10^{-13.833}$ , and  $K_{\text{a}}' = 10^{-4.3}$  (which may be compared to  $10^{-4.15}$  obtained by spectrophotometric titration of  $\text{Fl}_{\text{ox}}^+\text{CD}_3$ ). Below pH 3 ( $a_{\text{H}} \gg K_{\text{a}}'$ ,  $k_0 \gg k_{\text{HO}} K_{\text{w}}/a_{\text{H}}$ ), eq 6 reduces to

$$k_{\text{obsd}} = k_0 \quad (7)$$

Thus the upper plateau of Figure 4 describes the spontaneous rate. Between pH 6 and 8 ( $a_{\text{H}} \ll K_{\text{a}}'$ ,  $k_0 \ll k_{\text{HO}} K_{\text{w}}/a_{\text{H}}$ ), eq 8 applies,

$$k_{\text{obsd}} = k_{\text{HO}} K_{\text{w}} / K_{\text{a}}' \quad (8)$$

which defines the lower plateau. The determination of the first-order rate constants for the solvolysis of  $\text{Fl}_{\text{ox}}^+\text{CH}_3$  between pH 5 and 8 is complicated by the contribution to the observed spectral changes from the solvolysis of  $\text{FICH}_3$ , which is a product of the former reaction. The half-life of the latter reaction is inversely proportional to  $\text{FICH}_3$  concentration, since it is found to be second order in  $\text{FICH}_3$  species (see below). Therefore, it was possible to suppress  $\text{FICH}_3$  solvolysis by lowering the initial concentration of  $\text{Fl}_{\text{ox}}^+\text{CH}_3$ . At a concentration of  $\text{Fl}_{\text{ox}}^+\text{CH}_3$  of ca.  $10^{-5} \text{ M}$ , excellent first-order kinetics were obtained.

The solvolysis of  $\text{Fl}_{\text{ox}}^+\text{CH}_3$  was found to be subject to buffer catalysis. The second-order rate constants ( $k_{\text{gb}}$ ) for buffer catalysis were determined as follows: at a given pH, pseudo-first-order rate constants were obtained at several buffer concentrations and plotted against the total buffer concentration (Figure 5). The slope of the line obtained is given by

$$\text{slope} = k_{\text{gb}} \left( \frac{K_{\text{B}}}{K_{\text{B}} + a_{\text{H}}} \right) \left( \frac{a_{\text{H}}}{K_{\text{a}}' + a_{\text{H}}} \right) \quad (9)$$

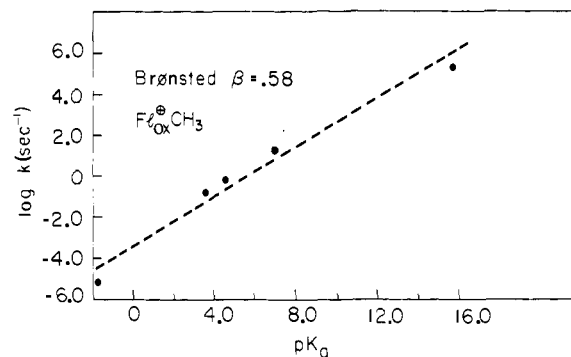


Figure 6. Bronsted plot for the general base-catalyzed solvolysis of  $\text{Fl}_{\text{ox}}^+\text{CH}_3$ . The points are for (in order of increasing  $\text{p}K_{\text{a}}$ )  $\text{H}_2\text{O}$ ,  $\text{HCO}_3^-$ ,  $\text{CH}_3\text{CO}_2^-$ ,  $\text{HPO}_4^-$ , and  $\text{HO}^-$ .

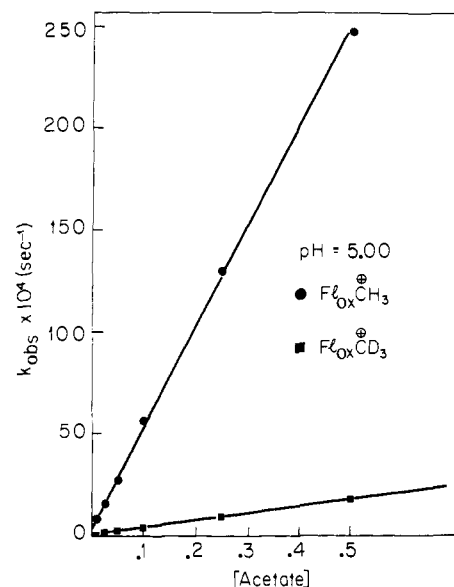


Figure 7. Observed first-order rate constants for the solvolysis of  $\text{Fl}_{\text{ox}}^+\text{CH}_3$  and  $\text{Fl}_{\text{ox}}^+\text{CD}_3$  as a function of total acetate buffer concentration (pH 5.00). The ratio of the slopes =  $(5.17 \times 10^{-2}) / (3.7 \times 10^{-3}) = k_{\text{H}}/k_{\text{D}} = 14.0$ .

where  $K_{\text{B}}$  is the acid dissociation constant of the buffer. With each buffer, three dilutions were made at three different pH's and secondary plots of (slope)  $(1 + (a_{\text{H}}/K_{\text{B}}))(K_{\text{a}}' + a_{\text{H}})$  vs.  $a_{\text{H}}$  were made (Figure 5). The slope of the line obtained is equal to  $k_{\text{gb}}$ . The rate constants ( $\text{M}^{-1} \text{ s}^{-1}$ ,  $30^\circ$ ,  $\text{H}_2\text{O}$ ,  $\mu = 1$  with KCl) and the  $\text{p}K_{\text{a}}$ 's of the conjugate acids of the bases studied are:  $\text{H}_2\text{O}$ ,  $\text{p}K_{\text{a}} = -1.74$ ,  $k_{\text{gb}} = 6.4 \times 10^{-6}$ ;  $\text{HCO}_3^-$ , 3.60,  $1.49 \times 10^{-1}$ ;  $\text{CH}_3\text{CO}_2^-$ , 4.60,  $6.48 \times 10^{-1}$ ;  $\text{HPO}_4^{2-}$ , 7.10, 15.5;  $\text{HO}^-$ , 15.74,  $2 \times 10^5$  ( $k_{\text{HO}}$  was obtained from the best fit to the pH-log  $k_{\text{obsd}}$  profile, and  $k_{\text{H}_2\text{O}}$  was obtained by dividing the spontaneous rate constant by 55.5). It should be pointed out here that these are only apparent rate constants. As will be made clear (see Discussion),  $k_{\text{gb}}$ 's should be divided by three to obtain the true second-order rate constants for reaction of base with  $\text{Fl}_{\text{ox}}^+\text{CH}_3$ . A Bronsted plot of the data is given in Figure 6 ( $\beta \approx 0.6$ ).

Since the reaction is buffer base catalyzed, the solvolysis of  $\text{Fl}_{\text{ox}}^+\text{CH}_3$  must occur via nucleophilic or general base catalysis. Comparison of the  $k_{\text{gb}}$  values for  $\text{Fl}_{\text{ox}}^+\text{CH}_3$  and  $\text{Fl}_{\text{ox}}^+\text{CD}_3$  when  $\text{H}_2\text{O}$  and  $\text{CH}_3\text{CO}_2^-$  serve as base provided isotope effects ( $k_{\text{H}}/k_{\text{D}}$ ) of 10.5 and 14.0, respectively (Figure 7). This result establishes the solvolysis of  $\text{Fl}_{\text{ox}}^+\text{CH}_3$  to occur via general base proton abstraction from the methyl group substituted upon the positively charged N(5) position in  $\text{Fl}_{\text{ox}}^+\text{CH}_3$ . The solvent deuterium kinetic isotope effect for solvolysis of  $\text{Fl}_{\text{ox}}^+\text{CH}_3$  was determined to be  $(k_{\text{H}_2\text{O}}/k_{\text{D}_2\text{O}} = 3.57 \times$

$10^{-4}/1.77 \times 10^{-4} = 2.0$  at pH = pD 2.0 (0.01 M HCl/H<sub>2</sub>O and 0.01 M DCl/D<sub>2</sub>O) in the absence of buffer. Since first-order kinetics were followed to 5 half-lives (correlation coefficients greater than 0.9998), exchange of substrate -H(D) with solvent does not occur. Similar solvent deuterium kinetic isotope effects have been obtained<sup>11</sup> with other carbon acids which lose a proton irreversibly in a rate-determining step.

It can be predicted (see Discussion) that in the presence of a suitable electron acceptor the observed rate constant for  $\text{Fl}_{\text{ox}}^+\text{CH}_3$  solvolysis should be one-third the value obtained in its absence. As will be made clear, benzoquinone is ideal as the electron acceptor. At pH 3.04 (0.06 M formate), the solvolysis of  $\text{Fl}_{\text{ox}}^+\text{CH}_3$  ( $10^{-4}$  M) in the presence of benzoquinone ( $4 \times 10^{-4}$  M) provides a value for  $k_{\text{obsd}}'$  of  $6.71 \times 10^{-4} \text{ s}^{-1}$ . When benzoquinone was absent,  $k_{\text{obsd}} = 2.02 \times 10^{-3} \text{ s}^{-1}$ . Thus, as predicted,  $k_{\text{obsd}}/k_{\text{obsd}}' = 3.0$ .

In the anaerobic reaction, the 5-methyl group in one-third of the  $\text{Fl}_{\text{ox}}^+\text{CH}_3$  molecules is converted to H<sub>2</sub>CO (Scheme III). This suggests that there is a carbinolamine intermediate on the reaction path, which breaks down to give H<sub>2</sub>CO and a flavin species. Based on the extensive literature<sup>12</sup> on carbinolamine formation, this is expected to be an equilibrium reaction. Therefore, if the solvolysis of  $\text{Fl}_{\text{ox}}^+\text{CH}_3$  is carried out in the presence of excess formaldehyde, further information may be obtained about the reaction mechanism. A kinetic run at pH 1.15 (with HCl), in the presence of 0.21 M formaldehyde, revealed that the observed rate is not influenced by H<sub>2</sub>CO. This result is consistent with Scheme III. Since 1,5-dihydro-3-methylumiflavin (FIH<sub>2</sub>) is likely to be an intermediate in the solvolysis of  $\text{Fl}_{\text{ox}}^+\text{CH}_3$  (see Discussion), the reaction of FIH<sub>2</sub> with  $\text{Fl}_{\text{ox}}^+\text{CH}_3$  was examined. At pH 7.14 FIH<sub>2</sub> ( $6.7 \times 10^{-5}$  M) reacts with  $\text{Fl}_{\text{ox}}^+\text{CH}_3$  (fourfold excess) during the mixing time of 15 s to give a 2:1 mixture of  $\text{FICH}_3\cdot$  and  $\text{Fl}_{\text{ox}}$ . Surprisingly, however, at pH 7.14 no reaction between another oxidized-reduced flavin pair,  $\text{Fl}_{\text{ox}}$  ( $7.4 \times 10^{-5}$  M) and  $\text{FIHCH}_3$  ( $2.4 \times 10^{-4}$  M) could be detected. After 2 days, there was no  $\text{FICH}_3\cdot$  production as judged by the absorbance at 585 nm.

**Hydrolysis of the Pseudo-Base of  $\text{Fl}_{\text{ox}}^+\text{CH}_3$  under Anaerobic Conditions (pH >8).** Above ca. pH 8 not all of the starting material is converted to a 2:1 mixture of  $\text{FICH}_3\cdot:\text{Fl}_{\text{ox}}$ . For instance, at pH 8.4 (in the absence of buffer) the maximum concentration of  $\text{FICH}_3\cdot$  produced corresponds to only ca. 30% of that obtained at pH values below 8 and, in addition, the reaction does not follow good first-order kinetics. At pH 9.93 (0.1 M carbonate buffer) no radical is detectable as product. Though the reaction is first order ( $k_{\text{obsd}} = 5.3 \times 10^{-4} \text{ s}^{-1}$ , followed at 350 nm) there is no deuterium isotope effect when  $\text{Fl}_{\text{ox}}^+\text{CD}_3$  is substituted for  $\text{Fl}_{\text{ox}}^+\text{CH}_3$ . A product with  $\lambda_{\text{max}}$  at ~308 nm is produced which upon exposure to air is converted to one absorbing at 322, 355 (sh), and 264 nm. Qualitatively, these observations parallel those made in studies of the hydrolysis of the flavin ring structure.<sup>13</sup> The dotted line of the pH-log  $k_{\text{obsd}}$  profile (Figure 4) was generated by use of eq 4 with the added extra term:

$$k_h \left( \frac{K_w}{a_H} \right) \left( \frac{K_a'}{K_a' + a_H} \right)$$

The value of the second-order hydrolysis rate constant,  $k_h$ , used to obtain the best fit was  $3.75 \text{ M}^{-1} \text{ s}^{-1}$ .

**Solvolysis of  $\text{FICH}_3\cdot$  under anaerobic conditions (pH 1–8)** obeys the rate equation

$$-\frac{d[\text{FICH}_3\cdot]}{dt} = k[\text{FICH}_3\cdot]^2 \quad (10)$$

From eq 10 it is apparent that the rate of disappearance of the radical is second order in that species. Thus, plots of  $[\text{FICH}_3\cdot]^{-1}$  vs. time are linear (Figure 8). The disappearance

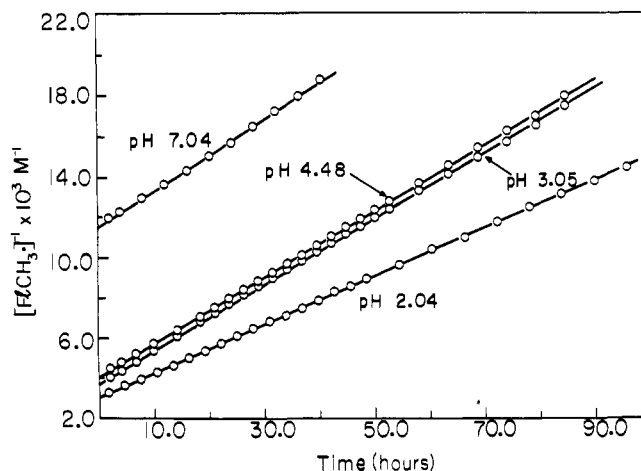


**Figure 8.**  $[\text{FICH}_3\cdot]^{-1}$  vs. time plots for  $\text{FICH}_3\cdot$  solvolysis. The initial concentrations of the radical (in order of increasing pH) were  $3.3 \times 10^{-4}$ ,  $2.8 \times 10^{-4}$ ,  $2.6 \times 10^{-4}$ , and  $8.8 \times 10^{-5}$  M.  $\text{FICH}_3\cdot$  was prepared by method 1 (see Table II).

of the radical was followed at 585 (above pH 2) and at 510 nm (below pH 2). The second-order rate constants obtained are given in Table II. Large primary deuterium kinetic isotope effects were observed when  $\text{FICD}_3\cdot$  was substituted for  $\text{FICH}_3\cdot$ . At pH 5 (0.1 M acetate),  $k_H/k_D = (7.5 \times 10^{-2} \text{ M}^{-1} \text{ s}^{-1})/(5.6 \times 10^{-3} \text{ M}^{-1} \text{ s}^{-1}) \approx 13$ , while at pH 7 (0.2 M phosphate),  $k_H/k_D = (8.7 \times 10^{-2} \text{ M}^{-1} \text{ s}^{-1})/(2.5 \times 10^{-3} \text{ M}^{-1} \text{ s}^{-1}) \approx 35$ . The solvent deuterium kinetic isotope effect for the solvolysis of  $\text{FICH}_3\cdot$  was determined,  $k_{\text{H}_2\text{O}}/k_{\text{D}_2\text{O}} = (3.4 \times 10^{-2} \text{ M}^{-1} \text{ s}^{-1})/(2.6 \times 10^{-2} \text{ M}^{-1} \text{ s}^{-1}) = 1.3$ , at pH 2.0 (0.01 M HCl/H<sub>2</sub>O and 0.01 M DCl/D<sub>2</sub>O). It is apparent from the rate constants given in Table II that the solvolysis of  $\text{FICH}_3\cdot$  is rather slow. For example, at one extreme, the first half-life for the solvolysis of a  $10^{-4}$  M solution of  $\text{FICD}_3\cdot$  at pH 7.0 is ca. 45 days. In obtaining the above isotope effects, we monitored 10–20% of the solvolysis of  $\text{FICD}_3\cdot$  and ca. 75% of that of  $\text{FICH}_3\cdot$ . At a given pH, comparison of the rates obtained with  $\text{FICH}_3\cdot$  prepared in situ from  $\text{Fl}_{\text{ox}}^+\text{CH}_3$  solvolysis (method 1 in Table II) and by comproportionation of  $\text{Fl}_{\text{ox}}^+\text{CH}_3$  and  $\text{FIHCH}_3$  (method 2 in Table II) reveals that in the latter case the observed rate constants are always higher by ca. 80%. We attribute the difference to a preequilibrium complexation of  $\text{FICH}_3\cdot$  with  $\text{Fl}_{\text{ox}}$  which slows down the rate.  $\text{Fl}_{\text{ox}}$  is initially present at a concentration half that of  $\text{FICH}_3\cdot$  when method 1 is used. The solvolysis of  $\text{FICH}_3\cdot$  prepared by method 2 is faster because there is no  $\text{Fl}_{\text{ox}}$  present in solution initially. With these considerations in mind, Table II further reveals that the solvolysis of  $\text{FICH}_3\cdot$  is not buffer-catalyzed and that  $k_{\text{obsd}}$  is independent of pH between 2.0 and 7.76. (Small differences observed when rate constants obtained by the same method are compared are likely to be due to specific ion effects.) These results are rather surprising in the light of the large primary deuterium kinetic isotope effects observed when  $\text{FICD}_3\cdot$  was substituted for  $\text{FICH}_3\cdot$  (see Discussion).

If  $\text{FICH}_3\cdot$  solvolysis is allowed to go on for some time and then ninhydrin is added, ca. 75% of  $\text{FICH}_3\cdot$  is regained. This result suggests that one of the products of  $\text{FICH}_3\cdot$  solvolysis is  $\text{FIHCH}_3$ , which is known<sup>14</sup> to react with ninhydrin to give  $\text{FICH}_3\cdot$ . Oxygenation can also be used to demonstrate the presence of  $\text{FIHCH}_3$ . However, it is difficult to quantitate the amount of radical formed by bubbling O<sub>2</sub> through the solution, because O<sub>2</sub> also reacts with the radical to give  $\text{Fl}_{\text{ox}}^+\text{CH}_3$  (see below). This complication is not encountered with ninhydrin.<sup>14</sup> There is yet another indication that  $\text{FIHCH}_3$  is a product. At pH 7, after about 2 half-lives (initial  $[\text{FICH}_3\cdot] \approx 1.6 \times 10^{-4}$  M), deviations from second-order kinetics are observed, the rate becoming faster. That this is due to the build up of

**Table II.** Second-Order Rate Constants for the Solvolysis of  $\text{FICH}_3$ ,<sup>a</sup>

pH	Buffer	Source of $\text{FICH}_3$ , <sup>b</sup>	Initial $[\text{FICH}_3]$	% reaction followed <sup>c</sup>	$k_{\text{obsd}} \text{ M}^{-1} \text{ s}^{-1}$ <sup>d</sup>
1.15	HCl	1	$1.7 \times 10^{-4}$	40	$\sim 7 \times 10^{-3}$
2.04	HCl	1	$3.3 \times 10^{-4}$	80	$3.4 \times 10^{-2}$
3.05	0.10 M formate	1	$2.8 \times 10^{-4}$	80	$4.6 \times 10^{-2}$
4.48	0.40 M formate	1	$2.6 \times 10^{-4}$	78	$4.6 \times 10^{-2}$
5.00	0.01 M acetate	1	$5.8 \times 10^{-5}$	Initial slope	$3.1 \times 10^{-2}$
5.00	0.025 M acetate	1	$1.1 \times 10^{-4}$		$3.0 \times 10^{-2}$
5.00	1.00 M acetate	1	$2.4 \times 10^{-4}$	74	$4.4 \times 10^{-2}$
6.54	0.20 M phosphate	1	$2.5 \times 10^{-4}$	32	$5.1 \times 10^{-2}$
7.04	0.25 M phosphate	1	$8.8 \times 10^{-5}$	39	$5.0 \times 10^{-2}$
7.76	0.039 M phosphate	1	$1.5 \times 10^{-4}$	56	$7.9 \times 10^{-2}$
5.00	0.10 M acetate	2	$1.6 \times 10^{-4}$	50	$7.5 \times 10^{-2}$
7.00	0.02 M phosphate	2	$1.6 \times 10^{-4}$	70	$7.8 \times 10^{-2}$
7.00	0.05 M phosphate	2	$1.6 \times 10^{-4}$	70	$8.5 \times 10^{-2}$
7.00	0.10 M phosphate	2	$1.6 \times 10^{-4}$	70	$7.9 \times 10^{-2}$
7.00	0.20 M phosphate	2	$1.7 \times 10^{-4}$	70	$8.7 \times 10^{-2}$
7.00	0.50 M phosphate	2	$1.4 \times 10^{-4}$	55	$9.5 \times 10^{-2}$
3.90	0.10 M formate	3	$3.1 \times 10^{-4}$	63	$4.6 \times 10^{-2}$

<sup>a</sup> Anaerobic, 30°,  $\text{H}_2\text{O}$ ,  $\mu = 1$  with KCl. <sup>b</sup>  $\text{FICH}_3$  made from (1)  $\text{Fl}_{\text{ox}}^+\text{CH}_3$  solvolysis; (2) comproportionation:  $\text{Fl}_{\text{ox}}^+\text{CH}_3 + \text{FIHCH}_3 \rightarrow 2 \text{FICH}_3$ ; (3)  $\text{FHMe} + \text{O}_2$  followed by deaeration. <sup>c</sup> The wavelength monitored was 585 nm at pH 2.04 and above, 510 nm at pH 1.15. <sup>d</sup>  $k_{\text{obsd}}$  was obtained as the slope of  $1/\text{OD}$  vs. time plot and converted to units of  $\text{M}^{-1} \text{ time}^{-1}$  by multiplying by the extinction coefficients at the given wavelength (pathlength of cell used = 1 cm).

$\text{FIHCH}_3$  in solution can be inferred from the following experiment: when  $\text{FIHCH}_3$  is added (fourfold excess) to a  $10^{-4}$  M  $\text{FICH}_3$  solution (pH 7.0), an immediate decrease ( $\sim 35\%$ ) in the radical absorption at 585 nm is observed, indicating complexation. The solvolysis of the radical under these conditions is several times faster, but is not second order. When  $\text{FIHCH}_3$  is not present at the start,  $\text{FICH}_3$  solvolysis is not effected by  $\text{FIHCH}_3$  produced in the reaction in an observable way until a critical concentration is reached. We therefore did not perform further experiments to quantitate the catalysis of  $\text{FICH}_3$  solvolysis by  $\text{FIHCH}_3$ . Another minor product of  $\text{FICH}_3$  solvolysis may be  $\text{Fl}_{\text{ox}}$ —a slight increase in absorbance at 443 nm accompanies the disappearance of the radical. The observed spectral changes are consistent with the stoichiometry of the equation



We have determined that at pH 5.0, the extinction coefficients ( $\text{M}^{-1} \text{ cm}^{-1}$ ) of  $\text{FICH}_3$  at 585 and 443 nm are 4200 and 2700, respectively. The  $\lambda_{\text{max}}$  of  $\text{FIHCH}_3$  is at 335 nm and it has a tail extending into the visible ( $\epsilon_{443} \sim 650$ ,  $\epsilon_{585} 0$ ).  $\text{Fl}_{\text{ox}}$  has a  $\lambda_{\text{max}}$  at 443 nm ( $\epsilon_{443} 12\ 000$ ). Using these extinction coefficients we can calculate that the increase in absorbance at 443 nm should be 18.8% of the decrease at 585 nm. Experimentally, there was observed ca. 17.3%, which agrees well with the calculated value. These results support eq 11. The overall mechanism of Scheme IV is proposed to account for these observations (see Discussion). In this scheme,  $\text{FIH}_2$  is generated from a complex between two radicals by a sequence of reactions.  $\text{FIH}_2$  then reacts with two radical species to give  $\text{Fl}_{\text{ox}}$  and two  $\text{FIHCH}_3$  (eq 32). Experimentally it was found that at pH 7,  $\text{FIH}_2$  (3-acetic acid derivative,  $2.06 \times 10^{-5}$  M) and  $\text{FICD}_3$  ( $6.14 \times 10^{-5}$  M) reacted during the mixing time of 15 sec. The final spectrum obtained indicated that all of the  $\text{FIH}_2$  had been converted to  $\text{Fl}_{\text{ox}}$  and that  $\text{FICD}_3$  was missing by an amount equivalent to twice the initial  $\text{FIH}_2$  concentration. These results support Scheme IV.

**Disappearance of  $\text{FICH}_3$  under anaerobic conditions (pH >8)** was found not to be second order in  $\text{FICH}_3$ , as is the case below pH 8 (followed at 585 nm). At pH 9.93 (0.1 M carbonate buffer), the time course of the solvolysis of  $\text{FICH}_3$  and

$\text{FICD}_3$  were found to be identical, so that a primary deuterium kinetic isotope effect (as seen below pH 8) is not apparent. Reduced flavin was a product as judged by the appearance of  $\text{FICH}_3$  (increase in absorbance at 585 nm) after bubbling  $\text{O}_2$  through the solution. Before making the solution aerobic, a peak at ca. 310 nm could be seen; after introduction of  $\text{O}_2$ , the final product had  $\lambda_{\text{max}}$ 's at 322, 355 (sh), and 264 nm. Apparently the decomposition of the radical is through the pseudo base ( $\text{FIOHCH}_3$ ) intermediate since the hydrolysis of  $\text{FIOHCH}_3$  provides product(s) of identical spectra (loc. cit.). Addition of  $\text{FICH}_3^-$  to  $\text{FICH}_3$  solutions was found to decrease the absorption of the radical at 585 nm, indicating complexation of the two species. For example,  $2 \times 10^{-4}$  M  $\text{FICH}_3$  solution has essentially zero absorbance in the presence of  $1.1 \times 10^{-3}$  M  $\text{FICH}_3^-$ . Thus, addition of  $\text{FICH}_3^-$  decreases the concentration of  $\text{FICH}_3$  in solution. The mixing of equimolar amounts of  $\text{FICH}_3^-$  and  $\text{Fl}_{\text{ox}}^+\text{CH}_3$  pseudo-base (pH 9.93, 0.1 M carbonate) so that the initial concentration of each species was  $1.2 \times 10^{-4}$  M, provided an increase of absorption at 585 nm ( $\text{FICH}_3$ ) which lasted ca. 7 min. A pseudo-first-order rate constant of  $10^{-2} \text{ s}^{-1}$  (correlation coefficient = 1.0000) was obtained for this reaction by using an  $\text{OD}_{\infty}$  ca. 4% higher than the maximum observed at 585 nm. Scheme II is consistent with the observation of first-order kinetics for this process. Assuming that  $k_2[\text{FICH}_3^-] \gg k_{-1}[\text{OH}^-]$  and that  $\text{Fl}_{\text{ox}}^+\text{CH}_3$  species is at a steady-state concentration, eq 12 is obtained.

$$\begin{aligned} d[\text{FICH}_3]/dt &= 2k_1[\text{FIOHCH}_3] \\ &= 2k_1[\text{FIOHCH}_3]_0 e^{-k_1 t} \end{aligned} \quad (12)$$

Thus,  $k_{\text{obsd}} = k_1 \approx 10^{-2} \text{ s}^{-1}$  at pH 9.93. Combination of eq 13 and 14 yields eq 15,

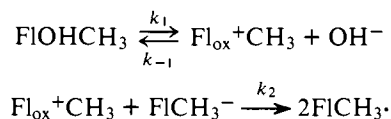
$$\frac{[\text{Fl}_{\text{ox}}^+\text{CH}_3][\text{OH}^-]}{[\text{FIOHCH}_3]} = \frac{k_1}{k_{-1}} \quad (13)$$

$$\frac{[\text{FIOHCH}_3][a_{\text{H}}]}{[\text{Fl}_{\text{ox}}^+\text{CH}_3]} = \frac{[\text{FIOHCH}_3]K_w}{[\text{Fl}_{\text{ox}}^+\text{CH}_3][\text{OH}^-]} = K_a' \quad (14)$$

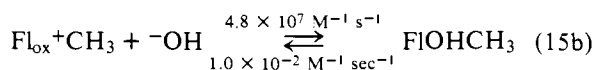
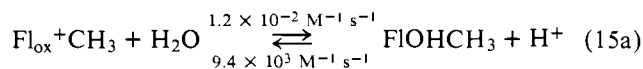
$$k_{-1} = k_1 K_a' / K_w \quad (15)$$

where  $K_a'$  is the pseudo-base formation equilibrium constant of  $\text{Fl}_{\text{ox}}^+\text{CH}_3$  determined by spectrophotometric titration. The rate of  $\text{OH}^-$  attack on  $\text{Fl}_{\text{ox}}^+\text{CH}_3$  to form the pseudo-base can

Scheme II



be obtained as  $4.8 \times 10^7 \text{ M}^{-1} \text{ s}^{-1}$  by substituting the values of  $k_1$ ,  $K_a'$ , and  $K_w$  ( $= 10^{-13.833}$ ) into eq 15. It is interesting to note that the rates of hydroxide attack on Schiff bases derived from benzophenone have been calculated<sup>15a</sup> to be ca. four orders of magnitude less than the value we obtain for the hydroxide attack on  $\text{Fl}_{\text{ox}}^+\text{CH}_3$ . The specific acid-catalyzed rate of conversion of  $\text{FlOHCH}_3$  to  $\text{Fl}_{\text{ox}}^+\text{CH}_3$  (reverse step of eq 4) was determined to be  $9.4 \times 10^3 \text{ M}^{-1} \text{ s}^{-1}$  by stopped flow experiments at pH 2.4. Utilizing this rate constant and the known equilibrium constant for the formation of  $\text{FlOHCH}_3$ , the rate of  $\text{H}_2\text{O}$  attack on  $\text{Fl}_{\text{ox}}^+\text{CH}_3$  can be calculated to be  $1.2 \times 10^{-2} \text{ M}^{-1} \text{ s}^{-1}$ . Thus the following rate constants pertain to the formation of the pseudo-base of  $\text{Fl}_{\text{ox}}^+\text{CH}_3$ :

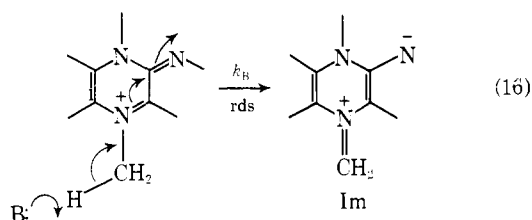


**$\text{FlCH}_3\cdot$  Solvolysis under Aerobic Conditions.**  $\text{FlCH}_3\cdot$  rapidly reacts with  $\text{O}_2$  to give  $\text{Fl}_{\text{ox}}^+\text{CH}_3$ , which is observable spectrally at pH's below 4, where the pseudo-base equilibrium does not interfere. This is confirmed further by comparing the time course of the solvolysis of  $\text{Fl}_{\text{ox}}^+\text{CH}_3$  prepared this way with that of authentic  $\text{Fl}_{\text{ox}}^+\text{CH}_3$ . They are found to be identical.

**Solvolysis of  $\text{Fl}_{\text{ox}}^+\text{CH}_3$  under aerobic conditions** was investigated in a cursory manner at pH 4.61, 3.05, and 2.04. The time it takes to convert all  $\text{Fl}_{\text{ox}}^+\text{CH}_3$  to product (which in this case is  $\text{Fl}_{\text{ox}}$  as identified by its spectrum) is longer aerobically than anaerobically. The reaction does not follow first-order kinetics unless the ratio of  $[\text{O}_2]/[\text{Fl}_{\text{ox}}^+\text{CH}_3]$  is maximized. Thus, when  $10^{-5} \text{ M}$   $\text{Fl}_{\text{ox}}^+\text{CH}_3$  in oxygen saturated  $10^{-3} \text{ M}$  HCl solution (no added KCl,  $\mu = 0.001$ ) is used, good first-order kinetics are observed. Under the same conditions the anaerobic first-order rate constant was found to be larger by a factor of 3.9 (anaerobic  $k_{\text{obsd}} = 4.54 \times 10^{-4} \text{ s}^{-1}$ , aerobic  $k_{\text{obsd}} = 1.16 \times 10^{-4} \text{ s}^{-1}$ ). Buffer catalysis could be detected in experiments carried out at pH 4.61 in various concentrations of air-saturated acetate solutions ( $\mu = 1$  with KCl,  $[\text{Fl}_{\text{ox}}^+\text{CH}_3] \approx 10^{-4} \text{ M}$ ). Under these conditions an initial buildup of  $\text{FlCH}_3\cdot$  could be observed. Kinetically the reactions were complex and were not further analyzed.

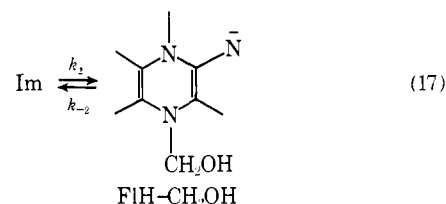
## Discussion

The findings of general base catalysis ( $\beta \approx 0.6$ ; Figure 6) and substantially lower reactivity of  $\text{Fl}_{\text{ox}}^+\text{CD}_3$  compared to  $\text{Fl}_{\text{ox}}^+\text{CH}_3$  (Figure 7) are conclusive evidence that the rate-determining step in the solvolysis of  $\text{Fl}_{\text{ox}}^+\text{CH}_3$  is the removal of a proton from the 5-methyl group (eq 16). That the reverse

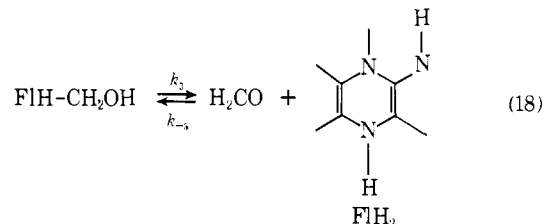


of this step may be unfavorable can be inferred from consideration of the electron rearrangement upon removal of the proton (eq 16) and is proven by the lack of exchange of -H for -D in  $\text{D}_2\text{O}$ . In analogy with the reactions of other imines,<sup>15</sup> the

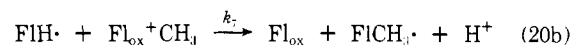
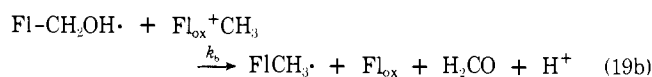
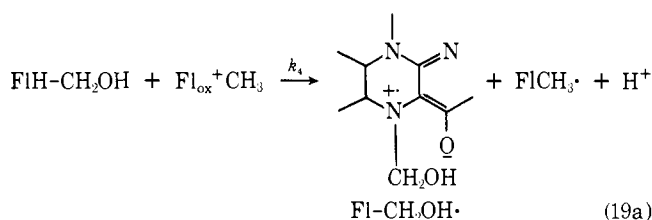
imine of eq 16 is expected to rapidly<sup>16</sup> form a carbinolamine (eq 17) by attack of  $\text{H}_2\text{O}$  or  $\text{HO}^-$ , and eliminate formaldehyde



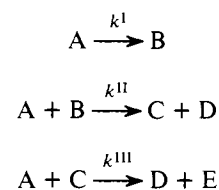
to give free amine, which in this case is 1,5-dihydro-3-methylflavin ( $\text{FIH}_2$  of eq 18). Both  $\text{FIH-CH}_2\text{OH}$ <sup>16</sup> and



$\text{FIH}_2$  (see Results) react with  $\text{Fl}_{\text{ox}}^+\text{CH}_3$  instantaneously to give  $\text{Fl}_{\text{ox}}$  and  $\text{FlCH}_3\cdot$  (eq 19a, 19b, 20a, 20b). Based on these con-

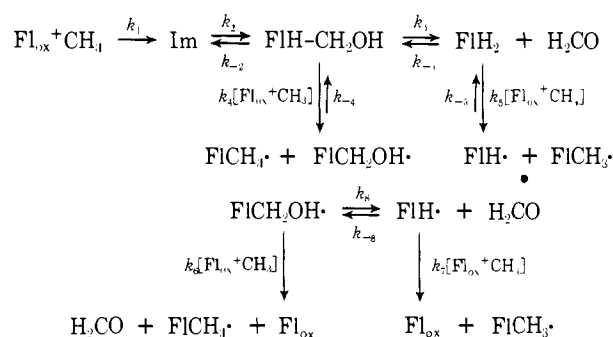


siderations, we propose Scheme III (where  $k_1 = k_{\text{B}}[\text{B}]$ ) to explain our results. For the sake of clarity it should be pointed out that Scheme III is of the following general form:



Comparison of the symbols reveals that A, B, C, D, and E represent  $\text{Fl}_{\text{ox}}^+\text{CH}_3$ ,  $\text{FIH-CH}_2\text{OH}$  and/or  $\text{FIH}_2$ ,  $\text{FlCH}_2\text{OH}\cdot$  and/or  $\text{FIH}\cdot$ ,  $\text{FlCH}_3\cdot$ , and  $\text{Fl}_{\text{ox}}$ , respectively. It is clear that a scheme of the above form predicts that the observed rate constant for the disappearance of A will be equal to  $3k^{\text{I}}$  if  $k^{\text{II}}$

Scheme III



and  $k^{11}$  are much larger than  $k^1$ . This is shown to be true for Scheme III also. Applying the steady-state approximation to the intermediates Im, FIH-CH<sub>2</sub>OH, FIH<sub>2</sub>, FI-CH<sub>2</sub>OH·, and FIH·, eq 21a-d are obtained,

$$[\text{FIH}_2] = \frac{k_1 k_3}{k_4 X + k_3 k_5} \quad (21a)$$

$$[\text{FIH-CH}_2\text{OH}] = \frac{k_1 X}{k_4 X + k_3 k_5} \quad (21b)$$

$$[\text{FIH}\cdot] = \frac{k_1(k_8(k_4 X + k_3 k_5) + k_3 k_5 k_6 [\text{Fl}_{\text{ox}}^+\text{CH}_3])}{(k_4 X + k_3 k_5)(k_6 Y + k_7 k_8)} \quad (21c)$$

$$[\text{FI-CH}_2\text{OH}\cdot] = \frac{k_1(k_4 X Y + k_3 k_5 k_{-8} [\text{H}_2\text{CO}])}{(k_4 X + k_3 k_5)(k_6 Y + k_7 k_8)} \quad (21d)$$

where  $X = k_5[\text{Fl}_{\text{ox}}^+\text{CH}_3] + k_{-3}[\text{H}_2\text{CO}]$  and  $Y = k_7[\text{Fl}_{\text{ox}}^+\text{CH}_3] + k_{-8}[\text{H}_2\text{CO}]$ . In arriving at eq 21a-d, we assumed that  $k_6[\text{Fl}_{\text{ox}}^+\text{CH}_3] \gg k_{-4}[\text{FICH}_3\cdot]$  and  $k_7[\text{Fl}_{\text{ox}}^+\text{CH}_3] \gg k_{-5}[\text{FICH}_3\cdot]$ . According to Scheme III, the rate of disappearance of  $\text{Fl}_{\text{ox}}^+\text{CH}_3$  is described by

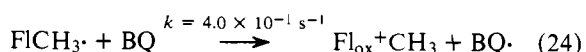
$$-d[\text{Fl}_{\text{ox}}^+\text{CH}_3]/dt = (k_1 + k_4[\text{FIH-CH}_2\text{OH}] + k_5[\text{FIH}_2] + k_6[\text{FI-CH}_2\text{OH}\cdot] + k_7[\text{FIH}\cdot])[\text{Fl}_{\text{ox}}^+\text{CH}_3] \quad (22)$$

Substituting the steady-state values of the intermediates into eq 22, one obtains the very simple result:

$$-d[\text{Fl}_{\text{ox}}^+\text{CH}_3]/dt = 3k_1[\text{Fl}_{\text{ox}}^+\text{CH}_3] \quad (23)$$

Thus,  $k_{\text{obsd}} = 3k_1$ . Since all the general base rate terms (Results, Figure 6) are subsets of  $k_1$ , it follows that the correct values of these constants are obtained by dividing the experimentally determined rate constants by three.

In arriving at eq 23, we made no assumptions regarding any step involving formaldehyde. Therefore, Scheme III agrees with experiment by predicting that  $k_{\text{obsd}}$  should not differ if the reaction is carried out in the presence of excess formaldehyde (see Results). A means of verifying the correctness of Scheme III and the conclusions derived from it would be obtained if the solvolysis of  $\text{Fl}_{\text{ox}}^+\text{CH}_3$  were studied in the presence of an electron acceptor which could: (a) oxidize the reduced flavin intermediates (FIH<sub>2</sub> and FIH-CH<sub>2</sub>OH) of Scheme III at a rate greater than that for the reaction of the latter with  $\text{Fl}_{\text{ox}}^+\text{CH}_3$ , and/or (b) convert  $\text{FICH}_3\cdot$  to  $\text{Fl}_{\text{ox}}^+\text{CH}_3$  at a rate much greater than that for proton abstraction ( $k_1$ ) from  $\text{Fl}_{\text{ox}}^+\text{CH}_3$ . If condition (a) and/or (b) is fulfilled, then Scheme III predicts that  $k_{\text{obsd}}$  should equal  $k_1$  and not  $3k_1$ . Benzoquinone (BQ) is ideal for this purpose since it has been reported to react with 1,5-dihydroriboflavin<sup>17</sup> and  $\text{FIHCH}_3$ <sup>14</sup> at what must be near diffusion-controlled rates (the estimates of second-order rate constants are  $>3.3 \times 10^7 \text{ M}^{-1} \text{ s}^{-1}$  and  $\geq 10^8 \text{ M}^{-1} \text{ s}^{-1}$ , respectively). Furthermore, BQ reacts with  $\text{FICH}_3\cdot$  to give  $\text{Fl}_{\text{ox}}^+\text{CH}_3$  ( $k_{\text{rate}} = 4.0 \times 10^{-1} \text{ s}^{-1}$ ). This latter reaction has been shown previously to be independent of  $[\text{BQ}]$  ( $[\text{BQ}] \geq 5[\text{FICH}_3\cdot]$ ) and pH.<sup>14</sup> The rate of proton abstraction ( $k_1$ ) from  $\text{Fl}_{\text{ox}}^+\text{CH}_3$  depends on the buffer and the buffer concentration used, however, with most of the conditions we employed,  $k_1$  was at least 100-fold less than  $4.0 \times 10^{-1} \text{ s}^{-1}$ . Therefore, BQ can certainly satisfy condition (b). Although benzoquinone is expected to react with the reduced flavin intermediates with a second-order rate constant  $>10^8 \text{ M}^{-1} \text{ s}^{-1}$ , it still may not be able to satisfy condition (a) totally, since the intermediates may also react with  $\text{Fl}_{\text{ox}}^+\text{CH}_3$  at diffusion-controlled rates. This is not a problem, however, since satisfaction of conditions (a) and (b) are kinetically equivalent. The kinetic derivation for case (b) is given below. In the presence of BQ we have the additional reaction:



If  $k_1 \ll 4.0 \times 10^{-1} \text{ s}^{-1}$ , we can apply the steady-state approximation to  $\text{FICH}_3\cdot$  (utilizing Scheme III, eq 21a-d and 24), and obtain

$$[\text{FICH}_3\cdot] = 2k_1[\text{Fl}_{\text{ox}}^+\text{CH}_3]/4.0 \times 10^{-1} \text{ s}^{-1} \quad (25)$$

Under the above stated conditions, the rate of disappearance of  $\text{Fl}_{\text{ox}}^+\text{CH}_3$  is given by

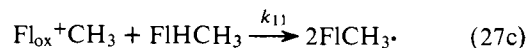
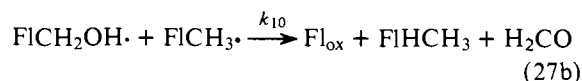
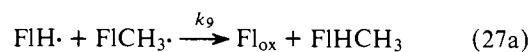
$$-d[\text{Fl}_{\text{ox}}^+\text{CH}_3]/dt = 3k_1[\text{Fl}_{\text{ox}}^+\text{CH}_3] - 4.0 \times 10^{-1} \text{ s}^{-1} [\text{FICH}_3\cdot] \quad (26a)$$

Substitution of eq 25 into 26a yields

$$-d[\text{Fl}_{\text{ox}}^+\text{CH}_3]/dt = k_1[\text{Fl}_{\text{ox}}^+\text{CH}_3] \quad (26b)$$

The validity of eq 26b is confirmed experimentally. At pH 3.04 (0.06 M formate) we obtained  $k_{\text{obsd}} = 2.02 \times 10^{-3} \text{ s}^{-1}$  in the absence of BQ. When BQ was present in fourfold excess over  $\text{Fl}_{\text{ox}}^+\text{CH}_3$ ,  $k_{\text{obsd}}' = 6.71 \times 10^{-4} \text{ s}^{-1}$ , hence substantiating that  $k_{\text{obsd}} = 3k_1$  and  $k_{\text{obsd}}' = k_1$ .

In Scheme III, the reactions described by eq 27a-c were omitted.



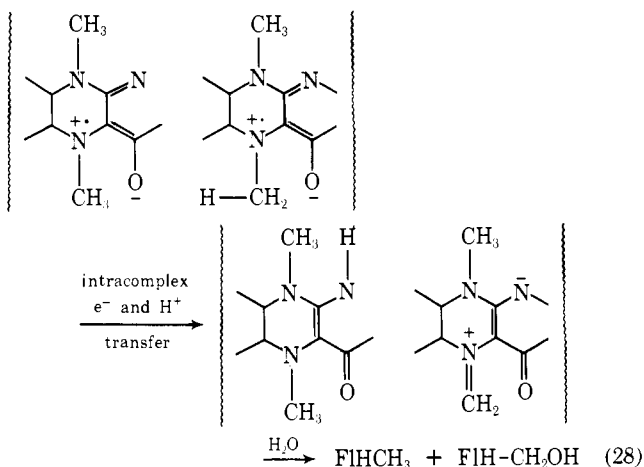
Our experimental results dictate that  $k_9$ ,  $k_{10}$ , and  $k_{11}$  represent effectively irreversible processes. We have found that  $\text{Fl}_{\text{ox}}$  and  $\text{FIHCH}_3$  do not react (pH 7.0) and that in the solvolysis of  $\text{FICH}_3\cdot$ ,  $\text{Fl}_{\text{ox}}^+\text{CH}_3$  is not an intermediate (see below). The  $k_9$  and  $k_{10}$  steps taken together with  $k_4$  and  $k_5$  steps of Scheme III would correspond to a two-electron reduction of  $\text{Fl}_{\text{ox}}^+\text{CH}_3$  to  $\text{FIHCH}_3$  by  $\text{FIH-CH}_2\text{OH}$  and  $\text{FIH}_2$ , respectively.  $\text{FIHCH}_3$  would then disproportionate with  $\text{Fl}_{\text{ox}}^+\text{CH}_3$  to give  $2\text{FICH}_3\cdot$  (eq 27c). There is no question that the reactions depicted in eq 27a-b can occur; however, it seemed more likely to us that the reaction of  $\text{FICH}_2\text{OH}\cdot$  or  $\text{FIH}\cdot$  with electron deficient  $\text{Fl}_{\text{ox}}^+\text{CH}_3$  would be more facile than the reaction of these two radicals with  $\text{FICH}_3\cdot$ . In any case, even if eq 27a-c are included in Scheme III, it can be shown that the overall result would be the same, i.e.,  $k_{\text{obsd}} = 3k_1$ .

The general base rate constants we have obtained, even when divided by three, reveal that  $\text{Fl}_{\text{ox}}^+\text{CH}_3$  ( $\log k_{\text{HO}^-} = 4.8$  at 30°) is comparable in acidity to carbon acids such as ethyl nitroacetate<sup>18</sup> ( $\log k_{\text{HO}^-} = 5.2$  at 25°) and acetylacetone<sup>19</sup> ( $\log k_{\text{HO}^-} = 4.6$  at 25°). It has been reported<sup>20</sup> that the 8-methyl group of FMN exchanges H for D in D<sub>2</sub>O at pH 6.8 (90-95 °C) with a rate constant of  $2.4 \times 10^{-4} \text{ s}^{-1}$ . At 30°, the rate of proton abstraction from  $\text{Fl}_{\text{ox}}^+\text{CH}_3$  by lyate species (pH 6.8) is ca.  $4.2 \times 10^{-3} \text{ s}^{-1}$ . Calculating the rate at 90° by assuming a two- to threefold increase in rate per 10 °C temperature increase reveals that the *N*<sup>5</sup>-methyl protons of  $\text{Fl}_{\text{ox}}^+\text{CH}_3$  are more acidic than the 8α protons of FMN by three to four orders of magnitude. The solvent deuterium kinetic isotope effect ( $k_{\text{H}_2\text{O}}/k_{\text{D}_2\text{O}}$ ) of 2.0 that is observed with  $\text{Fl}_{\text{ox}}^+\text{CH}_3$  is similar in magnitude to those obtained with other carbon acids which lose a proton irreversibly in a rate-determining step.<sup>11</sup> Primary deuterium isotope effects obtained for the ionization of carbon acids have been found to be dependent on the structure of the base used,<sup>21,22</sup>  $k_{\text{H}}/k_{\text{D}}$  increasing as the quantity  $\Delta pK = pK_{\text{SH}} - pK_{\text{BH}}$  (where SH is the carbon acid and B the base with which it reacts) decreases from positive values down to about zero, reaching a maximum at ca.  $\Delta pK = 0$ , and decreasing as  $\Delta pK$  becomes more negative. The isotope effects we obtained using  $\text{Fl}_{\text{ox}}^+\text{CH}_3$  and  $\text{Fl}_{\text{ox}}^+\text{CD}_3$  also showed dependence on the base used. Thus with H<sub>2</sub>O as the base  $k_{\text{H}}/k_{\text{D}} = 10.5$ , while the



acetate  $k_H/k_D = 14.0$ . Our results indicate, however, that proton removal from  $\text{Fl}_{\text{ox}}^+\text{CH}_3$  is effectively irreversible. Therefore, the increase in  $k_H/k_D$  we see with acetate cannot be correlated with  $\Delta pK$ . The phenomenon of tunneling<sup>21</sup> of the proton across the reaction coordinate barrier is undoubtedly involved as attested to by the magnitude of the isotope effects observed.

The disappearance of  $\text{FlCH}_3\cdot$  from solution is second order in this species. This is no ordinary disproportionation reaction as seen with ordinary 1,5-dihydroflavin [i.e.,  $2\text{FlH}\cdot \rightleftharpoons (\text{complex}) \rightleftharpoons \text{FlH}_2 + \text{Fl}_{\text{ox}}$ ].<sup>23</sup> The reaction with  $\text{FlCH}_3\cdot$  is consid-



erably faster than with  $\text{FlCD}_3\cdot$  ( $k_H/k_D \approx 13$  at pH 5.0,  $\sim 35$  at pH 7.0), indicating that, as in the case of  $\text{Fl}_{\text{ox}}^+\text{CH}_3$ , removal of a proton from the 5-methyl group is rate determining. The pH dependence of the isotope effect may not be real because the solvolysis rate of  $\text{FlCD}_3\cdot$  is so slow as to make an accurate measurement of a rate constant impractical. Our emphasis here is not on the absolute number but rather on the order of magnitude ( $k_H/k_D > 10$ ). Surprisingly, however, the reaction is not catalyzed by buffers and  $k_{\text{obsd}}$  is independent of pH between 2.0 and  $\sim 8.0$ , i.e., increasing  $[\text{HO}^-]$  by  $10^6$  causes no change in the rate. These three observations (lack of dependence of the rate on  $[\text{H}_3\text{O}^+]$ ,  $[\text{HO}^-]$ , and [buffer acids and bases] but large deuterium isotope effect) rule out any mechanism in which the  $N^5\text{-CH}_3$  proton is transported to an external base. Since radical disappearance is second order in this species, it is most logical to assume that C-H bond breaking occurs within a complex between two radicals. A mechanism consistent with the experimental results is provided in Scheme IV. In this scheme, C denotes the complex between two radicals and  $k_2$  refers to the rate of transfer of the elements of  $\text{H}\cdot + 1e^-$  from one radical to another within the complex. The imine and carbinolamine intermediates that form after the  $k_2$  step have been omitted for convenience, since the kinetic result obtained is the same whether they are included or not (see Scheme III). Applying the steady-state approximation to the intermediates  $\text{FlH}_2$  and  $\text{FlH}\cdot$ , the following results are obtained:

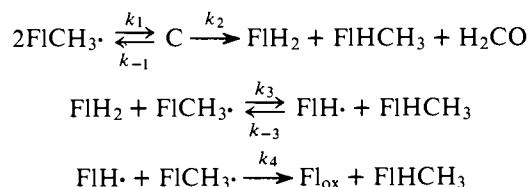
$$[\text{FlH}_2] = (k_2/k_3)K_1[\text{FlCH}_3\cdot] \quad (29)$$

$$[\text{FlH}\cdot] = (k_2/k_4)K_1[\text{FlCH}_3\cdot] \quad (30)$$

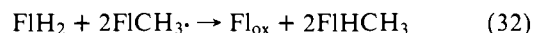
$$-d[\text{FlCH}_3\cdot]/dt = 2k_2[\text{C}] + k_3[\text{FlH}_2][\text{FlCH}_3\cdot] + k_4[\text{FlH}\cdot][\text{FlCH}_3\cdot] = 4k_2K_1[\text{FlCH}_3\cdot]^2 \quad (31)$$

In arriving at eq 29-31, it was assumed that  $k_{-1} \gg k_2$  (i.e., preequilibrium) and that  $k_4[\text{FlCH}_3\cdot] \gg k_{-3}[\text{FlHCH}_3]$ . These assumptions can be justified as follows: the rate of complex formation,  $k_1$ , is expected to be  $10^6\text{-}10^8 \text{ M}^{-1} \text{ s}^{-1}$ .<sup>23</sup> Since the equilibrium between the radical and the complex favors the radical,<sup>14</sup>  $k_{-1}$  must be considerably greater than  $k_2$ , which is

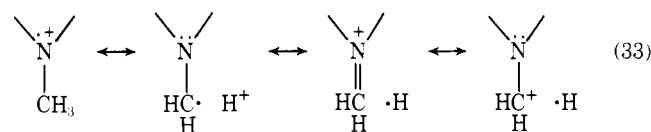
Scheme IV



the rate-determining step. The constant  $k_4$  is associated with a thermodynamically favorable process, since from two "unstable" radicals two stable products are formed. It is known that  $\text{Fl}_{\text{ox}}$  and  $\text{FlHCH}_3$  do not react or react very slowly (see Results). On the other hand, the reaction associated with  $k_{-3}$  is not expected to be exergonic. The free energy content of the products and the reactants of the  $k_3$  step are likely to be comparable. According to Scheme IV,  $\text{FlH}_2$  should react with  $\text{FlCH}_3\cdot$  at a rate greater than the rate of intracomplex proton (or  $\text{H}\cdot$ ) transfer, and the reaction should have the stoichiometry



Although we did not determine a rate constant for this process, we did observe that the mixing of  $\text{FlH}_2$  and  $\text{FlCD}_3\cdot$  solutions (pH 7.0) so that the concentrations after mixing were  $2.06 \times 10^{-5}$  and  $6.14 \times 10^{-5} \text{ M}$ , respectively, gave a final spectrum which indicated that a reaction with the stoichiometry of eq 32 had taken place during the mixing time of 15 s. These results are in complete agreement with Scheme IV. Alkyl group stabilization of nitrogen cation radicals has been suggested to be due to the contribution of the following resonance forms:<sup>24</sup>



The transfer of the elements of  $1e^- + \text{H}^+$  from one  $\text{FlCH}_3\cdot$  species to another may occur in a stepwise fashion or pertain to intracomplex transfer of  $\text{H}\cdot$ . Hydrogen atom transfer has recently been proposed to be of importance in the dihydroflavin reduction of carbonyl compounds to provide alcohols when the carbanion of the alcohol  $[\text{>}\ddot{\text{C}}\text{OH}]$  is highly unstable.<sup>25</sup>

**Acknowledgment.** This work was supported by a grant from the National Science Foundation.

## References and Notes

- (1) To be submitted in partial fulfillment of the requirements for the Ph.D. by C.K.
- (2) F. H. Westheimer in "The Mechanisms of Enzyme Action", W. D. McElroy and B. Glass, Ed., Johns Hopkins Press, Baltimore, Md., 1954, p 321.
- (3) P. Hemmerich and M. S. Jorns in "Enzyme Structure and Function", C. Veeger, J. Drenth, and R. A. Oosterban, Ed., North-Holland Publishing Co., Amsterdam, 1972, p 95.
- (4) G. A. Hamilton, *Prog. Bioorg. Chem.*, **1**, 83 (1971).
- (5) Sulfite and mercaptides represent highly polarizable nucleophiles. Sulfite is known to form both 5- and 4a-adducts with isoalloxazines and flavins [F. Müller and V. Massey, *J. Biol. Chem.*, **244**, 4007 (1969); L. Hevesi and T. C. Bruice, *Biochemistry*, **12**, 290 (1973)], and the oxidation of mercaptides has been established, within reasonable doubt, to involve intermediate 4a-addition [I. Yokoe and T. C. Bruice, *J. Am. Chem. Soc.*, **97**, 450 (1975); E. Loechler and T. Hollocher, *ibid.*, **97**, 3235 (1975)]. It is the opinion of this laboratory, however, that radical mechanisms are of prime concern in other flavin reactions as carbonyl group reduction (see ref 2).
- (6) D. Clerin and T. C. Bruice, *J. Am. Chem. Soc.*, **96**, 5571 (1974).
- (7) S. Ghisla, U. Hartman, P. Hemmerich, and F. Müller, *Justus Liebig's Ann. Chem.*, 1388-1415 (1973).
- (8) (a) L. Meites and T. Meites, *Anal. Chem.*, **20**, 984 (1948); (b) H. A. Itano, *Proc. Natl. Acad. Sci. U.S.A.*, **67**, 485 (1970).
- (9) T. C. Bruice and J. R. Maley, *Anal. Biochem.*, **34**, 275 (1970).
- (10) J. F. Walker, "Formaldehyde", 3d ed, Reinhold, New York, N.Y., 1964, p 486.
- (11) F. Hibbert and F. A. Long, *J. Am. Chem. Soc.*, **93**, 2836 (1971).
- (12) (a) W. P. Jencks, "Catalysis in Chemistry and Enzymology", McGraw-Hill, New York, N.Y., 1969; (b) J. M. Sayer, M. Peskin, and W. P. Jencks, *J. Am. Chem. Soc.*, **95**, 4277 (1973); (c) T. C. French and T. C. Bruice, *Biochemistry*, **3**, 1589 (1964); (d) J. M. Sayer, B. Pinsky, A. Schonbrunn, and

- W. Washtien, *J. Am. Chem. Soc.*, **96**, 7998 (1974); (e) R. N. F. Thorneley and H. Diebler, *ibid.*, **96**, 1072 (1974).
- (13) S. B. Smith and T. C. Bruice, *J. Am. Chem. Soc.*, **97**, 2875 (1975).
- (14) T. C. Bruice and Y. Yano, *J. Am. Chem. Soc.*, **97**, 5263 (1975).
- (15) (a) K. Koehler, W. Sandstrom, and E. H. Cordes, *J. Am. Chem. Soc.*, **86**, 2413 (1964); (b) N. Gravitz and W. P. Jencks, *ibid.*, **96**, 489 (1974).
- (16) R. F. Williams, S. Shinkai, and T. C. Bruice, submitted for publication.
- (17) M. J. Gibian and J. A. Rynd, *Biochem. Biophys. Res. Commun.*, **34**, 594 (1969).
- (18) R. P. Bell and D. J. Barnes, *Proc. R. Soc. London, Ser. A*, **318**, 421 (1970).
- (19) M. L. Ahrens, M. Eigen, W. Kruse, and G. Maass, *Ber. Bunsenges. Phys. Chem.*, **74**, 380 (1970).
- (20) F. J. Bullock and O. Jardetsky, *J. Org. Chem.*, **30**, 2056 (1965).
- (21) (a) R. P. Bell, "The Proton in Chemistry", 2d ed. Cornell University Press, Ithaca, N.Y., 1973, p 262; (b) *Chem. Soc. Rev.*, **3**, 513 (1974).
- (22) J. E. Dixon and T. C. Bruice, *J. Am. Chem. Soc.*, **92**, 905 (1970).
- (23) (a) B. G. Barman and G. Tollin, *Biochemistry*, **11**, 4760 (1972); (b) J. H. Swinehart, *J. Am. Chem. Soc.*, **87**, 904 (1965).
- (24) R. W. Taft, "Proton Transfer Reactions", E. F. Caldin and V. Gold, Ed., Chapman and Hall, London, 1975, p 64.
- (25) T. C. Bruice, *Prog. Bioorg. Chem.*, in press; R. F. Williams, S. Shinkai, and T. C. Bruice, *Proc. Natl. Acad. Sci. U.S.A.*, **72**, 1763 (1975).

## Conformational Interconversions of *cis,cis*-Cyclooctadiene-1,5

Otto Ermer

Contribution from the Abteilung für Chemie, Ruhr-Universität, D 463 Bochum, West Germany. Received September 9, 1975

**Abstract:** A detailed force-field study of conformational changes of *cis,cis*-cyclooctadiene-1,5 (I) is presented. A number of methodical points concerning the calculation of transition states and potential energy profiles are mentioned. All energy minimizations were performed by efficient and accurate Newton-Raphson techniques. Three potential energy minima and four transition states were found relevant for a description of the conformational properties of I. The transition states are characterized by their "transition coordinate"; i.e., by the eigenvector of the negative eigenvalue of the mass-weighted matrix of second derivatives of the potential energy. The seven calculated conformations are essentially characterized by different distributions of angle and torsional strain; the differences of the other strain factors are less pronounced. A complete set of thermodynamic properties was calculated. The most favorable calculated conformation of I is a twist-boat structure of symmetry  $C_2$  (C-CH<sub>2</sub>-CH<sub>2</sub>-C torsion angles 52.5°), in agreement with experimental evidence. Potential energy profiles for three different twist-boat/twist-boat interconversion processes were evaluated. The process via a twist transition state of  $D_2$  symmetry has the lowest calculated free enthalpy of activation ( $\Delta G^\ddagger = 4.15$  kcal mol<sup>-1</sup> at 100 K) and is suggested to interpret a <sup>1</sup>H NMR coalescence of I observed at 96 K ( $\Delta G^\ddagger = 4.4 \pm 0.1$  kcal mol<sup>-1</sup>) by Anet and Kozerski.<sup>1</sup> The other two processes [via a boat transition state ( $C_{2v}$  symmetry) and an intermediate chair minimum ( $C_{2h}$  symmetry), respectively] have calculated  $\Delta G^\ddagger$  values (at 100 K) of 5.73 and 5.91 kcal mol<sup>-1</sup>. Both the chair process and a combination of twist and boat processes are offered to explain a second observed <sup>1</sup>H NMR coalescence at 105 K ( $\Delta G^\ddagger = 4.9 \pm 0.1$  kcal mol<sup>-1</sup>).

Conformational changes of *cis,cis*-cyclooctadiene-1,5 (I) have recently been studied experimentally by Anet and Kozerski<sup>1</sup> (low-temperature NMR measurements) and computationally by Allinger and Sprague<sup>2</sup> (force-field calculations). We wish to report the results of another force-field study which are well compatible with the results and interpretations of Anet and Kozerski but less so with Allinger's and Sprague's calculations.

### Method

The method of calculation has been outlined in a recent publication.<sup>3</sup> The consistent force field used has also been described earlier.<sup>4</sup> Some further methodical points of interest are mentioned below where appropriate.

### Results

Altogether seven conformations were found important for a description of the conformational properties of I. Three correspond to potential energy minima ( $M_1$ ,  $M_2$ ,  $M_3$ ), four to one-dimensional partial maxima (saddle points, transition states:  $T_1$ ,  $T_2$ ,  $T_3$ ,  $T_4$ ). By applying Newton-Raphson iterations to suitable starting geometries, the internal parameters of Figure 1 were obtained. The final average absolute derivatives of the potential energy  $V$  with respect to the Cartesian atomic coordinates were in all cases less than  $10^{-6}$  kcal mol<sup>-1</sup> Å<sup>-1</sup>. Vibrational frequencies and principal moments of inertia were calculated and used for the evaluation of the thermodynamic properties of Table I. Calculated potential energy paths relating the minima and transition states of Figure 1 are given in Figures 2-4.

### Discussion

**Potential Energy Minima.** The available experimental evidence indicates that the most favorable conformation of I in the gas phase<sup>5</sup> and in solution<sup>1</sup> is the twist-boat form of symmetry  $C_2$  ( $M_1$ , Figure 1), in agreement with Allinger's and Sprague's and our calculations. This conformation was also observed in the crystals of two derivatives of I, namely, *syn*-3,7-dibromo-*cis,cis*-cyclooctadiene-1,5 (II)<sup>6</sup> and (*all-ax*)-4,8-dimethyl-*cis,cis*-cyclooctadiene-1,5-dicarboxamide-3,7 (III).<sup>7</sup> The ring geometries observed in these two crystals are also given in Figure 1. It appears that in both cases the eight-ring boats are more twisted than calculated for I [C-CH<sub>2</sub>-CH<sub>2</sub>-C torsion angles observed for II and III are 65° and 76° (average), respectively (Figure 1); calculated 52.5° (Figure 1); calculated by Allinger and Sprague, 37.9°<sup>2</sup>]. To what degree this difference reflects the various intra- and intermolecular perturbations exerted on the conformation of the eight-membered ring by the substituents (and the other packing forces) in the crystals of II and III cannot be decided from the results of the calculations presented here. It can be said, however, that the energy difference of the eight-ring conformations in the crystals of II and III, and our calculated geometry is rather small (see below).  $M_1$  is characterized by a low torsional energy yet appreciable angle strain (Table I) which originates from a transannular H...H repulsion (Figure 1; corresponding calculated H...H distance, 1.992 Å). Another manifestation of this interaction is an abnormally high calculated symmetric CH<sub>2</sub>-scissoring frequency (A-mode) of 1560 cm<sup>-1</sup>. MacNicol et al.<sup>6</sup> interpret an observed band of solid II at 1487 cm<sup>-1</sup> as this unusual scissoring vibration.